



Feasibility of ultrafast dynamic magnetic resonance imaging for the diagnosis of axillary lymph node metastasis: A case report

Yuka Kikuchi^a, Mio Mori^{a,*}, Tomoyuki Fujioka^a, Emi Yamaga^a, Goshi Oda^b,
Tsuyoshi Nakagawa^b, Anri Koyanagi^c, Shohei Tomii^d, Kazunori Kubota^e, Ukihide Tateishi^a

^a Department of Diagnostic Radiology, Tokyo Medical and Dental University, 1-5-45 Yushima, Bunkyo-ku, Tokyo 113 - 8510, Japan

^b Department of Surgery, Breast Surgery, Tokyo Medical and Dental University, 1-5-45 Yushima, Bunkyo-ku, Tokyo 113 - 8510, Japan

^c Department of Comprehensive Pathology, Tokyo Medical and Dental University, 1-5-45 Yushima, Bunkyo-ku, Tokyo 113 - 8510, Japan

^d Department of Pathology, Medical Hospital, Tokyo Medical and Dental University, 1-5-45 Yushima, Bunkyo-ku, Tokyo 113 - 8510, Japan

^e Department of Radiology, Dokkyo Medical University, 880 Kitakobayashi, Shimotsugun Mibumachi, Tochigi 321-0293, Japan

ARTICLE INFO

Keywords:

Breast cancer
Axillary lymph node metastasis
Nodal staging
Dynamic contrast-enhanced breast magnetic resonance imaging
Ultrafast dynamic magnetic resonance imaging

ABSTRACT

A 74 year old Japanese woman was diagnosed with invasive breast carcinoma. Her axillary lymph node was slightly swollen and had a short-axis diameter of 8 mm, but fine-needle aspiration did not lead to the diagnosis of metastasis. Subsequent 18F-fluorodeoxyglucose positron emission tomography/computed tomography showed no abnormal accumulation on the lymph node. Ultrafast dynamic magnetic resonance imaging yielded a very fast contrast enhancement like that of the primary lesion based on which we suspected lymph node metastasis. To our knowledge, this is the first report that shows that ultrafast imaging has contributed to the diagnosis of axillary lymph node metastasis.

1. Introduction

The lymph node status is one of the most important prognostic factors in breast cancer and is used to guide locoregional and systemic treatment decisions [1]. If the node metastases are diagnosed preoperatively, neoadjuvant chemotherapy is considered as a treatment option and sentinel lymph node biopsy (SLNB) can be omitted. However, for the definitive detection of axillary lymph node (ALN) metastases, there is currently no other modality than SLNB [2]. Thus, various imaging techniques have been reported in the effort to improve the diagnostic accuracy.

Ultrafast dynamic magnetic resonance imaging (MRI) is a novel dynamic contrast-enhanced MRI (DCE-MRI) approach. High-spatiotemporal resolution can be achieved with acceleration techniques, such as parallel imaging, view-sharing, or compresses sensing [3–6]. With this technique, kinetic information in the very early phase of

contrast enhancement—that is particularly useful for breast cancer diagnosis—has been acquired. It is commonly accepted that ultrafast imaging is useful in the diagnosis of breast cancer itself, but its contribution to lymph node metastases is still unknown. Herein, we report a case in which ultrafast imaging was useful for the diagnosis of ALN metastases. To the best of our knowledge, this is the first report wherein ultrafast imaging has contributed to the diagnosis of ALN metastases.

2. Case presentation

Our medical ethics committee approved this retrospective study and waived the requirement for written informed consent. A 74 year old Japanese woman with a palpable mass on her left breast was referred to our hospital. Mammography showed an irregular, indistinct, partially spiculated mass without calcification (Fig. 1). The ultrasonogram showed an irregular hypoechoic mass in the 10 o'clock position of the

Abbreviations: SLNB, sentinel lymph node biopsy; ALN, axillary lymph node; MRI, magnetic resonance imaging; DCE-MRI, dynamic contrast-enhanced MRI; VAB, vacuum assisted breast biopsy; FNA, fine-needle aspiration; [F-18]FDG PET/CT, 18F-fluorodeoxyglucose positron emission tomography/computed tomography; SUVmax, maximum standardized uptake value; T1WIFS, T1-weighted fat-suppressed; VIBRANT, volume imaged breast assessment; FOV, field-of-view; CNB, core needle biopsy.

* Corresponding author.

E-mail addresses: y.yashima89@gmail.com (Y. Kikuchi), m.mori.116@yahoo.co.jp (M. Mori), fjokmrad@tmd.ac.jp (T. Fujioka), ymgdrnm@tmd.ac.jp (E. Yamaga), oda.srg2@tmd.ac.jp (G. Oda), nakagawa.srg2@tmd.ac.jp (T. Nakagawa), koyanagi.pth2@tmd.ac.jp (A. Koyanagi), tomiph1@tmd.ac.jp (S. Tomii), kbtmrad@tmd.ac.jp (K. Kubota), ttisdrnm@tmd.ac.jp (U. Tateishi).

<https://doi.org/10.1016/j.ejro.2020.100261>

Received 13 August 2020; Accepted 24 August 2020

2352-0477/© 2020 The Author(s).

Published by Elsevier Ltd.

This is an open access article under the CC BY-NC-ND license

(<http://creativecommons.org/licenses/by-nc-nd/4.0/>).

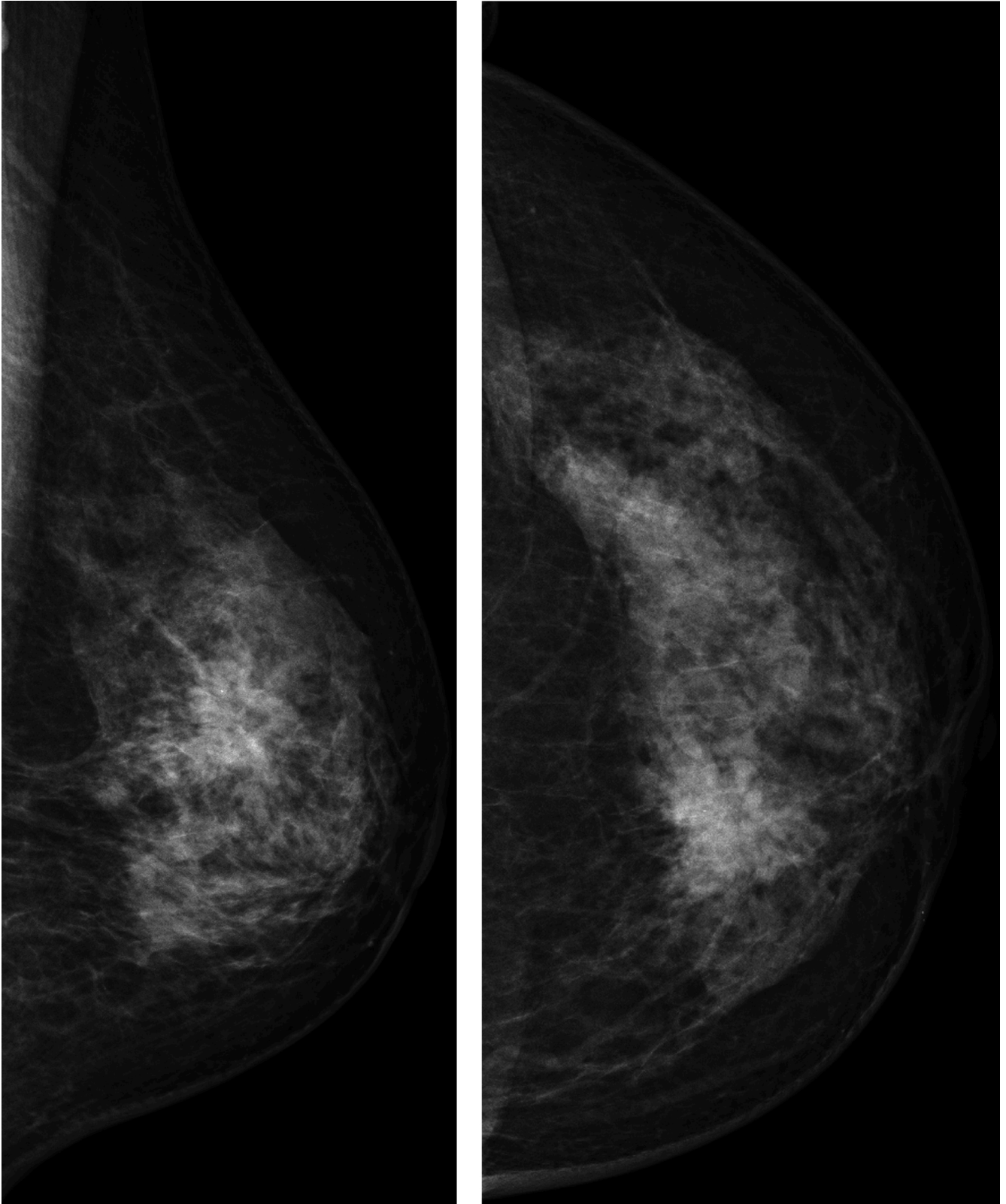


Fig. 1. Mammography of the left breast. Mammography shows an irregular, indistinct, partially spiculated mass with a diameter of 29 mm at the (a) upper-middle mediolateral oblique view, and at (b) middle-medial craniocaudal view. No calcification is detected.

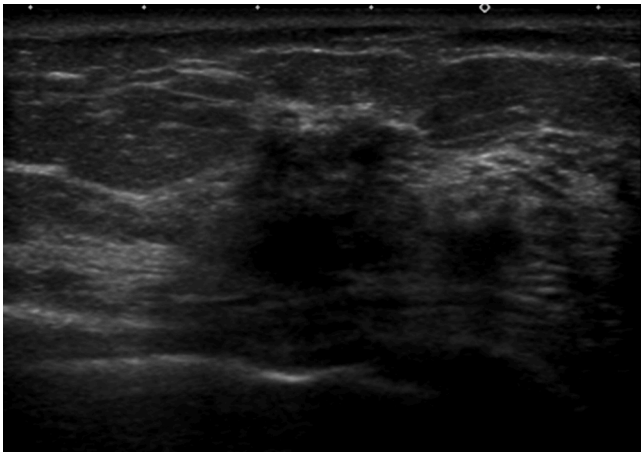


Fig. 2. Ultrasonography of the left breast. Ultrasonography shows an irregular hypoechoic mass with indistinct margin and posterior shadowing at the 10 o'clock position of the left breast. Its size is 26 × 14 × 16 mm.

left breast (Fig. 2). In the left axilla, there was an 18 × 8 mm node with an eccentric cortical thickening at level I (Fig. 3).

The patient had undergone ultrasonogram-guided, 12G, vacuum assisted breast biopsy (VAB) and fine-needle aspiration (FNA) of the left ALN at level I. Breast biopsy revealed the luminal type of invasive carcinoma, and FNA cytology showed suspicious cells with abnormal features (Class III). 18F-fluorodeoxyglucose positron emission tomography/computed tomography ([F-18]FDG PET/CT) yielded a minor uptake in the left breast mass [maximum standardized uptake value (SUV_{max}) = 1.7]. Owing to the equivocal uptake of the left ALN at level I after FNA (SUV_{max} = 1.4), we could not conclude whether the test was positive for metastasis (Fig. 4).

Subsequently, DCE-MRI was performed to determine a surgical plan with a 3.0 T MRI (Signa Pioneer, General Electric Medical Systems, Milwaukee, WI, USA). The patients were scanned in the prone position using a 16-channel phased-array bilateral breast coil (NeoCoil 3.0 T 16-channel breast coil, General Electric Medical Systems, Milwaukee, WI, USA). High-resolution, three-dimensional longitudinal relaxation T1-weighted fat-suppressed (T1WIFS) gradient-echo sequence with volume imaged breast assessment (VIBRANT) acquisitions were conducted before and after the injection of gadobutrol (Gadovist, Bayer Healthcare,

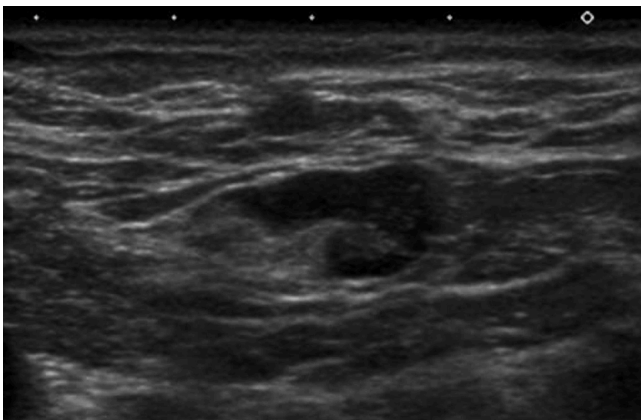


Fig. 3. Ultrasonography of the left axillary lymph node. Ultrasonography showed a lymph node with an eccentric cortical thickening at the left level of the axilla.

Berlin, Germany) at a dose of 0.1 mM/kg and a rate of 1.0 ml/s followed by a 30 ml saline flush at a rate of 1.0 ml/s. Immediately after the acquisition of precontrast T1WIFS, a series of 17 ultrafast acquisitions were interleaved before the first postcontrast phase of conventional DCE-MRI. The injection of contrast agent began simultaneously with the onset of ultrafast imaging. Differential subsampling with the Cartesian ordering technique—the combination of VIBRANT sequence and view sharing method—was used for the ultrafast acquisition (gradient echo, field-of-view (FOV): 360 mm, slice thickness: 4 mm, matrix: 360 × 340 mm, repetition time/echo time: 3.7/1.3 ms, flip angle: 10°, slice thickness: 4.0 mm, spacing: 2.0 mm, and a temporal resolution of 5.2 s per frame, 17 frames). The dynamic sequences were preceded by a T1-weighted sequence and a diffusion-weighted series, and were followed by a T2-weighted sequence as part of our clinical routine protocol. MRI showed an irregular breast mass with a fast initial enhancement surrounded by small masses and a clumped enhancement in the upper inner quadrant of the left breast. This primary tumor was enhanced from the 8th phase of the ultrafast series. We also detected an enhancing ipsilateral ALN with cortical thickening at level I. It was enhanced from the 7th phase of the ultrafast series at a much earlier stage than other lymph nodes on the ipsilateral and the contralateral axilla (Fig. 5a and b). These findings increased the suspicion of ALN metastasis. A 16G core needle biopsy (CNB) by ultrasonography revealed ALN metastasis.

The patient underwent three-week hormonal therapy and subsequent left mastectomy and left axillary nodal dissection. A breast specimen revealed invasive lobular carcinoma with scattered lobular carcinoma in situ (Fig. 6a). The patient had 16 of the 28 ALN metastases with the extranodal invasion at levels I and II (Fig. 6b). Of the metastatic lymph nodes, the largest has a size of 14 × 8 mm.

3. Discussion

In this study we reported a case in which ultrafast dynamic MRI was useful for the diagnosis of ALN metastasis. The ALN exhibited cortical thickening on ultrasonogram, but accumulation on [F-18]FDG PET/CT was equivocal and difficult to diagnose. The CNB was added based on the findings of the ultrafast dynamic MRI and the diagnosis of the ALN metastasis was reached preoperatively.

In clinical, node-negative patients with a stage T1 or T2 breast cancer, SLNB is now the standard staging procedure. However, it has been reported that SLNB has a false-negative rate in the range of 0–29% [7], and it requires many medical resources and complicated procedures [8]. In addition, ultrasonography-guided FNA is also associated with false negatives, and a meta-analysis reported their sensitivity and specificity to be 70–78% and 100%, respectively [9]. There is a need for accurate diagnostic imaging that would allow the use of techniques other than SNLB.

Although mammography and ultrasonography have conventionally been used to diagnose lymph node metastases, the accuracy is not so high. Walsh et al. reported that the sensitivity and specificity of detection of malignant ALN on mammography were 31% and 97%, respectively, when a length greater than 33 mm was used as a predictor of malignancy [10]. Hwang et al. reported that the sensitivity and specificity on ultrasonogram for T1 breast cancer were 88.7% and 44.6%, respectively, when the following characteristics were used as predictors of malignancy: cortical thickening or eccentric cortical lobulation with obliteration of the echogenic hilum, irregular shape, loss of fatty hilum, or round shape [2].

[F-18]FDG PET/CT is capable to perform functional evaluations based on glucose metabolism in addition to morphology, and is useful for assessing regional lymph node status and identifying distant metastases. However, despite its high specificity, its sensitivity for the detection of ALN metastasis is relatively poor, especially in small lesion cases because of spatial resolution limits. Robertson et al. reported that [F-18]FDG PET/CT has a sensitivity of 60% and a specificity of 97% in detecting lymphatic metastases [11]. In addition, a smaller

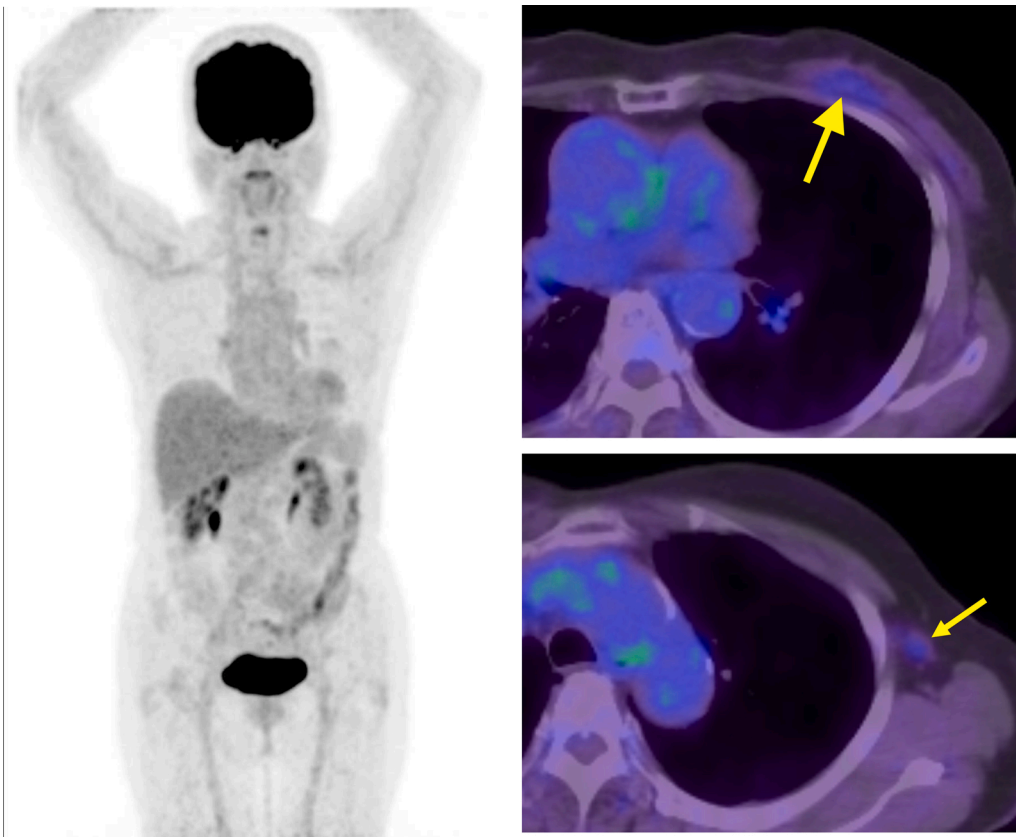


Fig. 4. Whole body 18F-fluorodeoxyglucose positron emission tomography/computed tomography ([F-18]FDG PET/CT).

(a) Minimum-intensity projection, whole-body PET image. (b) Cross-section of the primary lesion, PET/CT. (c) Cross-section of the axillary lymph node, PET/CT. [F-18]FDG accumulation was slight in both primary lesion and axillary lymph node metastases (maximum standardized uptake values of 1.7 and 1.4, respectively, see arrows).

accumulation has been documented in cases of invasive lobular carcinoma compared with invasive ductal carcinoma. The same effects are expected for ALN [12].

Breast MRI is extensively used for diagnosis, evaluation of multiplicity, and extent of tumors in the breast, monitoring the response of chemotherapy, and screening of women with high breast cancer risk. Ultrafast dynamic MRI is a very high-spatiotemporal resolution protocol executed in the early postcontrast period that enables the acquisition of the early inflow of contrast in lesions that are diagnostically important. Several reports have demonstrated that the kinetic assessment of ultrafast imaging has comparable or higher diagnostic ability than that of standard imaging in the benign/malignant diagnosis of breast lesions [3–6]. Conversely, there are no prior reports that evaluated the diagnostic ability for ALN metastases on ultrafast dynamic MRI.

In our case, we suspected ALN metastasis based on its slight cortical thickening on ultrasonogram but FNA failed to diagnose. The accumulation of the ALN on [F-18]FDG PET/CT was equivocal probably because its glucose metabolic rate was not so high. On ultrafast dynamic MRI, ALN showed very fast inflow similar to that of the primary lesion that led us to the suspicion of metastasis. We have shown that ultrafast dynamic MRI may be useful for the evaluation of primary breast lesions and for the diagnosis of ALN metastases. However, ultrafast dynamic MRI was superior to [F-18]FDG PET/CT in our case, but all other axillary lymph node metastases could not be detected. Micrometastases or ALNs outside the FOV may be difficult to detect. Further studies with more cases are required.

4. Conclusions

We presented a case in which ultrafast dynamic MRI was useful for diagnosing ALN metastasis. Use of the technique provided evidence for possible ALN metastasis based on the very early enhancement that was similar to the primary breast lesions. Ultrafast dynamic MRI may be useful for the evaluation of primary breast lesions and for the diagnosis of ALN metastasis.

Funding

None declared.

Ethical approval details

This study has been approved by the research ethics committee of Tokyo Medical and Dental University, Registration number: M2019-137.

Declaration of competing interest

None declared.

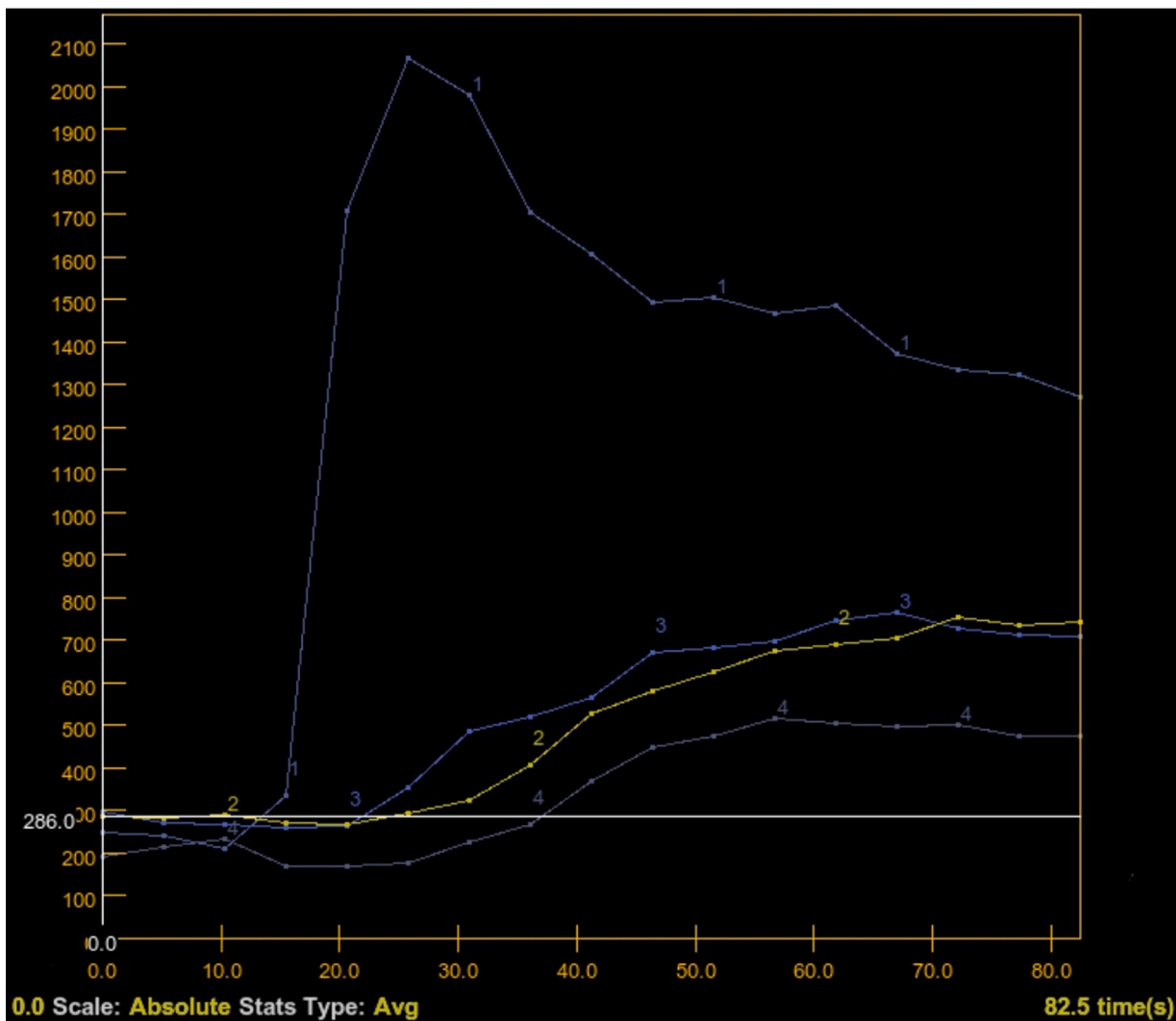
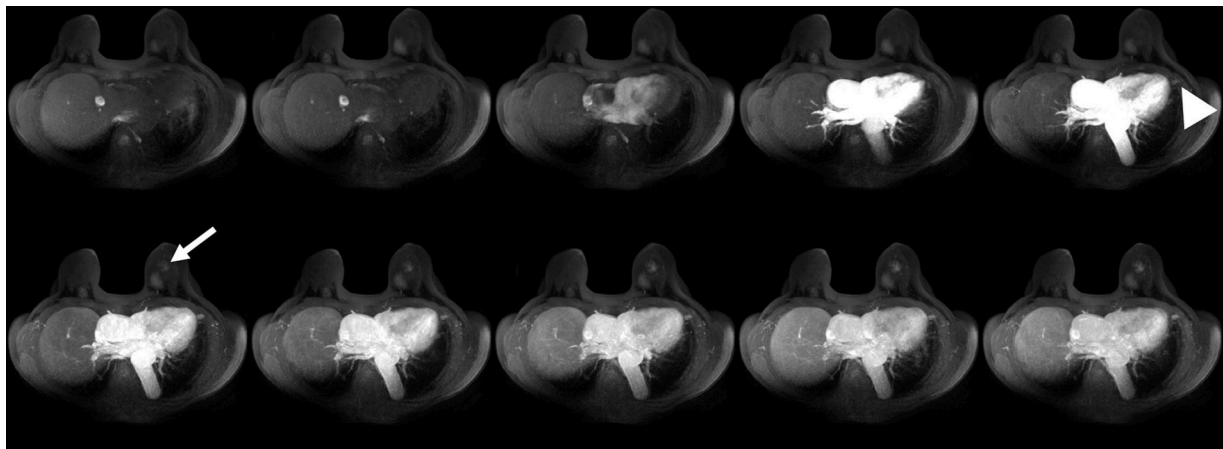


Fig. 5. Ultrafast dynamic MRI.

(a) Minimum-intensity projection (MIP), fat-suppressed T1-weighted image (FST1WI), precontrast, 1st, 3rd, 5th, 7th (upper row, from left to right), 9th, 11th, 13th, 15th, 17th (lower row, from left to right) phase of ultrafast dynamic series.

Breast lesion begins to be enhanced from the 8th phase of the ultrafast dynamics study (arrow) and the left axillary lymph node begins from the 7th phase (arrowhead). Ultrafast dynamic MRI does not show other ipsilateral and contralateral axillary lymph nodes.

(b) Time-intensity curves of aorta (1), breast lesion (2), metastatic left axillary lymph node (3), and normal lymph node of the right axilla (4) based on the ultrafast dynamic series.

The left metastatic lymph node enhanced much earlier than a normal lymph node.

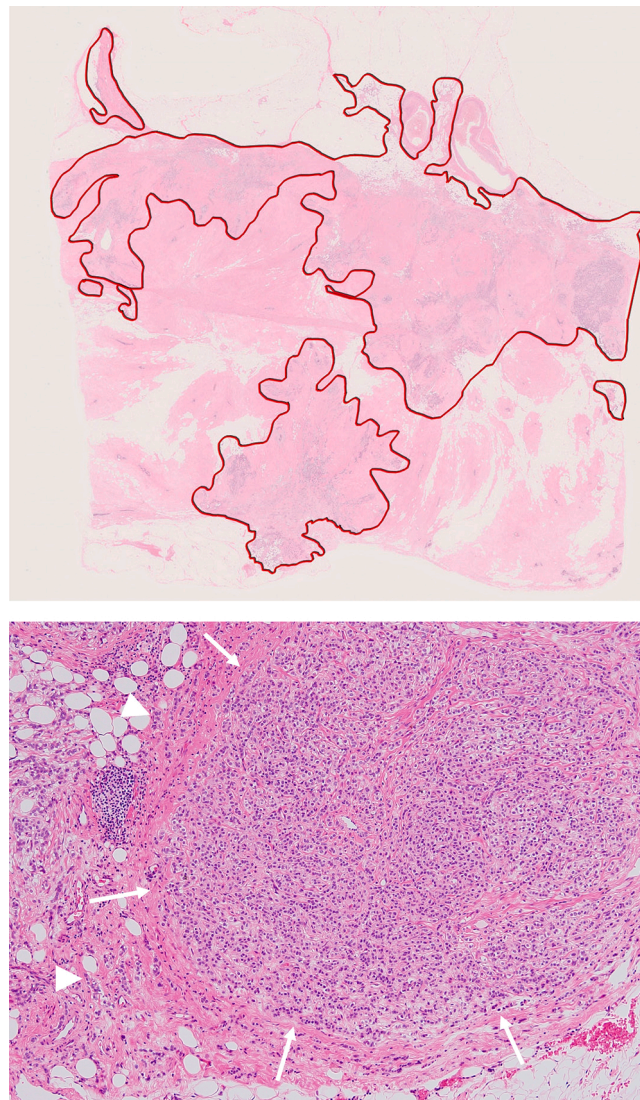


Fig. 6. Histopathology of the left breast cancer and the axillary lymph node.

(a) Shows an invasive lobular carcinoma of the breast (hematoxylin-eosin stain, loupe).

(b) Shows axillary lymph node metastasis (hematoxylin-eosin stain, original magnification, $\times 10$). The tumor cells show the same morphologic features as the primary lesion (arrows). An extranodal extension is observed (arrowheads).

References

- [1] S.W. Beenken, M.M. Urist, Y. Zhang, et al., Axillary lymph node status, but not tumor size, predicts locoregional recurrence and overall survival after mastectomy for breast cancer, *Ann. Surg.* 237 (2003) 732–739, <https://doi.org/10.1097/01.SLA.0000065289.06765.71>.
- [2] S.O. Hwang, S.W. Lee, H.J. Kim, W.W. Kim, H.Y. Park, J.H. Jung, The comparative study of ultrasonography, contrast-enhanced MRI, and (18)F-FDG PET/CT for detecting axillary lymph node metastasis in T1 breast cancer, *J. Breast Cancer* 16 (2013) 315–321, <https://doi.org/10.4048/jbc.2013.16.3.315>.
- [3] R.M. Mann, R.D. Mus, van J. Zelst, C. Geppert, N. Karssemeijer, B. Platel, A novel approach to contrast-enhanced breast magnetic resonance imaging for screening: high-resolution ultrafast dynamic imaging, *Invest. Radiol.* 49 (2014) 579–585, <https://doi.org/10.1097/RLI.0000000000000057>.
- [4] H. Abe, N. Mori, K. Tsuchiya, et al., Kinetic analysis of benign and malignant breast lesions with ultrafast dynamic contrast-enhanced MRI: comparison with standard kinetic assessment, *AJR Am. J. Roentgenol.* 207 (2016) 1159–1166, <https://doi.org/10.2214/AJR.15.15957>.
- [5] R.D. Mus, C. Borelli, P. Bult, et al., Time to enhancement derived from ultrafast breast MRI as a novel parameter to discriminate benign from malignant breast lesions, *Eur. J. Radiol.* 89 (2017) 90–96, <https://doi.org/10.1016/j.ejrad.2017.01.020>.
- [6] M. Honda, M. Kataoka, N. Onishi, et al., New parameters of ultrafast dynamic contrast-enhanced breast MRI using compressed sensing, *J. Magn. Reson. Imaging* 51 (2020) 164–174, <https://doi.org/10.1002/jmri.26838>.
- [7] T. Kim, A.E. Giuliano, Lyman G.H., Lymphatic mapping and sentinel lymph node biopsy in early-stage breast carcinoma: a metaanalysis, *Cancer* 106 (2006) 4–16, <https://doi.org/10.1002/cncr.21568>.
- [8] A.D. Purushotham, S. Upponi, M.B. Klevesath, et al., Morbidity after sentinel lymph node biopsy in primary breast cancer: results from a randomized controlled trial, *J. Clin. Oncol.* 23 (2005) 4312–4321, <https://doi.org/10.1200/JCO.2005.03.228>.
- [9] I. Balasubramanian, C.A. Fleming, M.A. Corrigan, H.P. Redmond, M.J. Kerin, A. J. Lowery, Meta-analysis of the diagnostic accuracy of ultrasound-guided fine-needle aspiration and core needle biopsy in diagnosing axillary lymph node metastasis, *Br. J. Surg.* 105 (2018) 1244–1253, <https://doi.org/10.1002/bjs.10920>.
- [10] R. Walsh, P.J. Kornguth, M.S. Soo, R. Bentley, D.M. DeLong, Axillary lymph nodes: mammographic, pathologic, and clinical correlation, *AJR Am. J. Roentgenol.* 168 (1997) 33–38, <https://doi.org/10.2214/ajr.168.1.8976915>.
- [11] I.J. Robertson, F. Hand, M.R. Kell, FDG-PET/CT in the staging of local/regional metastases in breast cancer, *Breast* 20 (2011) 491–494, <https://doi.org/10.1016/j.breast.2011.07.002>.
- [12] S. Ueda, H. Tsuda, H. Asakawa, et al., Clinicopathological and prognostic relevance of uptake level using 18F-fluorodeoxyglucose positron emission tomography/computed tomography fusion imaging (18F-FDG PET/CT) in primary breast cancer, *Jpn. J. Clin. Oncol.* 38 (2008) 250–258, <https://doi.org/10.1093/jjco/hyn019>.